

# Injectable and Biodegradable pH-Responsive Hydrogels for Localized and Sustained Treatment of Human Fibrosarcoma

Liubing Li,<sup>†,#</sup> Jun Gu,<sup>†,#</sup> Jie Zhang,<sup>‡,§,#</sup> Zonggang Xie,<sup>†</sup> Yufeng Lu,<sup>†</sup> Liqin Shen,<sup>†</sup> Qirong Dong,<sup>\*,†</sup> and Yangyun Wang<sup>\*,‡,§</sup>

<sup>†</sup>The Second Affiliated Hospital of Soochow University, 1055 Sanxiang Road, Suzhou, 215004, Jiangsu, China

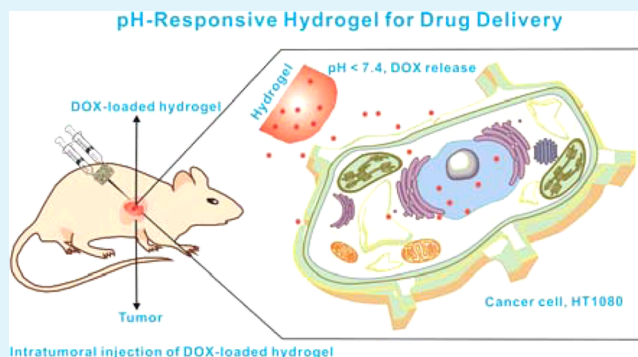
<sup>‡</sup>School for Radiological & Interdisciplinary Sciences (RAD-X), and School of Radiation Medicine and Protection, Soochow University, Suzhou, 215123, Jiangsu, China

<sup>§</sup>Collaborative Innovation Center of Radiation Medicine of Jiangsu Higher Education Institutions, 199 Renai Road, Suzhou Industrial Park, Suzhou, 215123, Jiangsu, China

## S Supporting Information

**ABSTRACT:** Injectable hydrogels are an important class of biomaterials, and they have been widely used for controlled drug release. This study evaluated an injectable hydrogel formed *in situ* system by the reaction of a polyethylene glycol derivative with  $\alpha,\beta$ -polyaspartylhydrazide for local cancer chemotherapy. This pH-responsive hydrogel was used to realize a sol–gel phase transition, where the gel remained a free-flowing fluid before injection but spontaneously changed into a semisolid hydrogel just after administration. As indicated by scanning electron microscopy images, the hydrogel exhibited a porous three-dimensional microstructure. The prepared hydrogel was biocompatible and biodegradable and could be utilized as a pH-responsive vector for drug delivery. The therapeutic effect of the hydrogel loaded with doxorubicin (DOX) after intratumoral administration in mice with human fibrosarcoma was evaluated. The inhibition of tumor growth was more obvious in the group treated by the DOX-loaded hydrogel, compared to that treated with the free DOX solution. Hence, this hydrogel with good syringeability and high biodegradability, which focuses on local chemotherapy, may enhance the therapeutic effect on human fibrosarcoma.

**KEYWORDS:** injectable, pH-responsive hydrogel, chemotherapy, drug delivery, human fibrosarcoma



## INTRODUCTION

In the past few decades, injectable hydrogels have been widely used as drug delivery and implant materials, because of their outstanding characteristics of nonoperative therapeutics to the patients.<sup>1–5</sup> Injectable hydrogels can be classified into physical and chemical gels on the basis of their gelation mechanism: the former and latter are formed by reversible noncovalent or covalent interactions, respectively.<sup>6–9</sup> Since the noncovalent interactions in physical gels are sensitive to the surrounding environment, it is convenient to induce sol–gel transitions in physical gels by changing temperature, solvent, or pH.<sup>10–13</sup> In comparison to physical hydrogels, chemical hydrogels demonstrate better mechanical strength;<sup>14</sup> however, they are less widely used, because of the low-molecular-weight cross-linkers, initiators, and residual catalysts used during their preparation, which often exhibit high toxicity.<sup>15–17</sup> Because of the aforementioned reasons, it is challenging to integrate the excellent stability of chemical gels and good stimuli responsiveness of physical gels into a single gel system.<sup>18</sup>

Meanwhile, dynamic covalent chemistry is attractive for the preparation of these materials,<sup>19</sup> which utilizes dynamic

covalent bonds for the preparation of the products rather than noncovalent interactions. The constitution and physicochemical properties of the products can be adjusted by reforming the thermodynamically controlled reactions of these dynamic covalent bonds. As a result, the products behave as supramolecular entities that are responsive to external stimuli. Nevertheless, they are more stable than the common supramolecular entities, because of the strength of the covalent bonds that are formed.<sup>20–23</sup> Recently, Schiff base formation has been reported to be a fascinating approach for the preparation of injectable hydrogels. This approach has received significant attention because of the efficient and orthogonal formation of imine bonds between the amino groups and aldehyde groups under physiological conditions without any external additive.<sup>24–26</sup> Along with imine bonds, acylhydrazone bonds have also been successfully utilized to prepare dynamic covalent polymers.<sup>27,28</sup> Generally, acylhydrazone bonds can be formed

Received: January 14, 2015

Accepted: April 2, 2015

Published: April 2, 2015

in mildly acidic solutions or neutral solutions using catalytic aniline;<sup>29</sup> these conditions are analogous to the physiological environments in the body.<sup>30,31</sup> In view of this characteristic, these bonds can be utilized for the *in situ* formation of hydrogels for biomedical applications.

Human fibrosarcoma is a soft tissue sarcoma and often occurs in the limbs. Typical treatment methods include surgery, chemotherapy, and radiotherapy, with chemotherapy being the primary treatment for fibrosarcoma patients.<sup>32,33</sup> However, the systemic administration of chemotherapeutic drugs is typically associated with severe toxicity, because these drugs cannot be selectively accumulated in the cancer cells as well as they can be rapidly cleared from the body.<sup>5</sup> Fortunately, this issue can be completely solved by local administration, through which anticancer drugs can be directly transported to the cancer sites.<sup>10,34</sup> Moreover, compared to systemic administration, local administration can significantly maintain drug concentrations at high levels in tumor areas while reducing the toxicity to the normal tissues and organs.<sup>35,36</sup> Currently, for all local administration systems, intratumoral injectable *in situ* forming gel systems are gaining increasing attention. These injectable systems exhibit many advantages such as tumor specificity and prolonged retention in the body, as well as catering to specific patient preference.<sup>5,37</sup> In addition, they can be locally administered as liquids, which later rapidly change into gels in the tumor sites as drug reservoirs. Hence, the use of intratumoral injectable gels formed *in situ* is a prospective approach for the development of local chemotherapeutic drug delivery systems.

In this study, we designed and synthesized a new injectable hydrogel based on polyethylene glycol (PEG) dialdehyde and  $\alpha,\beta$ -polyaspartylhydrazide. We have also evaluated the gel system formed *in situ*, and more specifically, a doxorubicin (DOX)-containing pH-responsive hydrogel for local chemotherapy. By mixing the PEG dialdehyde solution with a solution of  $\alpha,\beta$ -polyaspartylhydrazide solution, a chemically cross-linked hydrogel can be easily formed *in situ*. The efficacy of this system was evaluated for the treatment of human fibrosarcoma in mice.

## ■ EXPERIMENTAL SECTION

**Chemicals and Reagents.** Poly(succinimide) (PSI) (polydispersity index = 1.4, molecular weight = 2.1 kDa) was synthesized in-house according to refs 38 and 39. Hydrazine hydrate aqueous solution (80%), tetrahydrofuran (THF), and *N,N*-dimethyl-formamide (DMF) were purchased from Shanghai Civi Chemical Technology Co., Ltd. Poly(ethylene glycol) (PEG,  $M_w$  = 2000 Da), *p*-formyl benzoic acid, *N,N'*-dicyclohexylcarbodiimide (99%) and 4-(dimethylamino) pyridine (99%) were purchased from Sigma–Aldrich (Shanghai, China). Doxorubicin hydrochloride (DOX·HCl) was obtained from Beijing Huafeng United Technology Co., Ltd. THF was distilled over sodium before use. All the other reagents used were analytical reagent grade.

**Synthesis of Benzaldehyde-Terminated PEG (DF-PEG).** DF-PEG was prepared according to the previous report.<sup>24</sup> To a solution of PEG2000 (3.26 g, 1.63 mmol) in dry THF (100 mL), DMAP (0.050 g), *p*-formyl benzoic acid (0.98 g, 6.52 mmol) and *N,N'*-dicyclohexylcarbodiimide (1.68 g, 8.15 mmol) was added. After being stirred at 25 °C for 24 h under nitrogen atmosphere, white solid was generated and filtered, then precipitated with diethyl ether. The rough product was repeatedly dissolved in THF and precipitated in diethyl ether three times and finally a white solid was obtained. The

product was dried under reduced pressure at room temperature and 3.12 g of DF-PEG was collected in 82.9% yield.

**Synthesis of Polyaspartylhydrazide (PAHy).** PAHy was prepared from PSI based on the previous references with very minor modification.<sup>40,41</sup> To a solution of PSI (3 g) in DMF (40 mL), 4.8 mL of hydrazine hydrate ( $98.76 \times 10^{-3}$  mol) in DMF (5 mL) was added slowly. The mixture was maintained at 25 °C for 4 h using a water bath, when a precipitate was observed. This solid was filtered and washed several times with acetone. The raw polymer was redissolved into distilled water and dialyzed thoroughly against distilled water. The final polymer was freeze-dried and maintained at 4 °C.

**Measurements.** <sup>1</sup>H NMR spectra were obtained on a Varian Unity Model INOVA 400NB spectrometer (in D<sub>2</sub>O). Fourier transform infrared spectra (FT-IR) were obtained using Bruker Model VERTEX80 spectrophotometer at room temperature. Three-dimensional (3D) microstructures of the prepared hydrogel and degraded hydrogel were observed by scanning electron microscopy (SEM) when samples were freeze-dried and coated with gold. The experiment was carried out on a Model Atm3030 SEM system (Hitachi, Tokyo, Japan).

**Hydrogel Formation.** A PAHy solution (3%, w/w) was obtained by dissolving PAHy into phosphate buffer saline (PBS). DF-PEG (1.0 g) was dissolved in 4.0 g of PBS to form a DF-PEG solution (20%, w/w). Equal volume of PAHy and DF-PEG solutions in PBS were injected into a vial using a commercially available 3 mL 1:1 fibriJet applicator assembly (Shanghai Misawa Medical Industry Co., Ltd.). The precursor mixture solutions in the vials then were kept in a water bath at 37 °C and the gelation time was counted using a vial inverting method. The hydrogels in the full paper were prepared similarly, according to the above procedure.

**pH-Responsive Ability of the Injectable Hydrogel.** To demonstrate pH-responsive ability of the hydrogel upon stimulus, experiments were done according to the following procedure. The gel was first prepared, in which small amount of DOX was added for better tracking. Saturated HCl solution (60  $\mu$ L, 12 M) was added to the gel for liquefaction in about 15 min with vortex. The addition of concentrated NaOH solution (60  $\mu$ L, 12 M) was able to regenerate hydrogel in  $\sim$ 60 s. The sol–gel transitions adjusted by HCl or NaOH solutions can be repeated at least five times.

**DOX Loading and *In Vitro* DOX Release.** DOX-loaded hydrogels were obtained in three vials by mixing 3% PAHy solution (0.50 mL), 20% DF-PEG solution (0.50 mL), and DOX aqueous solution (5  $\mu$ L, 40 mg/mL) with a vortex for  $\sim$ 30 s. The prepared samples were kept at 37 °C for 6 h; then, buffer solutions at pH 7.4 (10 mL), pH 5.0 (10 mL), and pH 6.0 (10 mL) were added to three vials separately. The control group was obtained by mixing PAHy solution (0.50 mL), pure water (0.50 mL), and DOX aqueous solution (5  $\mu$ L, 40 mg/mL), and the absorbance of the control group at 485 nm was referenced as 100%. The vials were shaken at a rate of 120 rpm in darkness at 37 °C. At a specified time, the released medium (4 mL) was collected for measurement and 4 mL of fresh buffer was readded. The DOX release amount from gels was determined by absorbance at 485 nm. The *in vitro* cumulative DOX release can be calculated using the following equation:

$$\text{cumulative DOX released} = V_e \sum_{i=1}^{n-1} C_i + V_0 C_n$$

where  $V_e$  is the volume of released solution collected for each time point (4 mL),  $V_0$  is the volume of origin buffer solutions (10 mL),  $C_i$  is the DOX concentration in the release medium at displacement time  $i$ , and  $n$  is the total times of displacement.  $C_n$  is the final DOX concentration in the released medium. The data obtained represent the mean value of three replicates with a standard deviation ( $\pm$ SD).

**Biocompatibility Evaluation.** NIH-3T3 cells and HT1080 cell were used to investigate the biocompatibility of the injectable hydrogel using MTT assay. Normally, the number of surviving cells is directly proportional to the level of mitochondrial dehydrogenation of viable cells, which can form blue formazan crystals from MTT. The mixed polymer solution was obtained by mixing the same volume of precursor PAHy and DF-PEG polymer solutions. NIH-3T3 cells and HT1080 cells were seeded in 96-well plates at an initial density of 8000 cells/well in a DMEM medium with 10% FBS. After 24 h, the cells were dosed with fresh DMEM medium mixed polymeric solution at concentrations of 0–2 mg/mL. The cells were further incubated for 48 h and culture medium was removed and replaced with MTT solution for 4 h. The MTT solution was discarded and DMSO was added to each well to dissolve the formazan crystals. Absorbance of the dissolved formazan crystals was recorded by a microplate reader (BioTek, Synergy NEO, America) at 570 nm. The relative cell viability was calculated by comparing the absorbance in control wells with culture medium only. The data shown are the mean value of six replicates with a standard deviation ( $\pm$ SD).

**Evaluation of Gel Formation *In Vivo*.** To evaluate the possibility of gel formation *in vivo*, subcutaneous injection of 100  $\mu$ L 3% (w/w) PAHy PBS solution and 100  $\mu$ L 20% (w/w) DF-PEG PBS solution into female BALB/c mice using a commercially available 3 mL 1:1 fibrijet applicator assembly was investigated. Ten minutes later, the injection site was cut open and the morphology of the hydrogel in that area was observed and recorded.

**Antitumor Efficacy of the DOX-Loaded Hydrogel.** Animal experiments were approved by the Institutional Animal Care and Use Committee of Soochow University. Female BALB/c nude mice (16–18 g) 7 weeks old were obtained from Model Animal Research Center of Nanjing University (Nanjing, China) at least 1 week before experimental commencement. Briefly, HT1080 cells ( $5 \times 10^6$  cells per mouse) were injected into the flanks of female mice subcutaneously. When the tumors reached a size of  $\sim$ 500 mm<sup>3</sup> (about 15 days after transplantation), the time was designated day 0. Mice ( $n = 3$  per group) were divided into three groups and received saline control, free DOX solution, and the DOX-loaded hydrogel treatments, respectively. A total dose equivalent to 10 mg/kg of DOX for free DOX and DOX-loaded hydrogel was administered intratumorally. The tumor sizes along with the change in body weight of each mouse were recorded every 2 days. The tumor volume ( $V$ ) was obtained using the following equation:

$$V = \frac{ab^2}{2}$$

where  $a$  and  $b$  were the tumor measurements at the widest and longest points, respectively.

**Ex Vivo Histological Staining.** At day 20, mice were anesthetized and tumors were removed and immersed in 4% buffered paraformaldehyde for 48 h, and then embedded in paraffin. The paraffin-embedded tissue samples of the

implanted tumor were sliced at a thickness of 5 mm, and stained with hematoxylin and eosin (H&E) for histopathological changes evaluated by microscopy (Nikon, Model TE2000U).

## RESULTS AND DISCUSSION

**Polymer Synthesis.** PEG was treated with *p*-formylbenzoic acid to afford a dibenzaldehyde-functionalized polymer (DF-PEG) (Figure 1a). Figure 1b shows the <sup>1</sup>H NMR

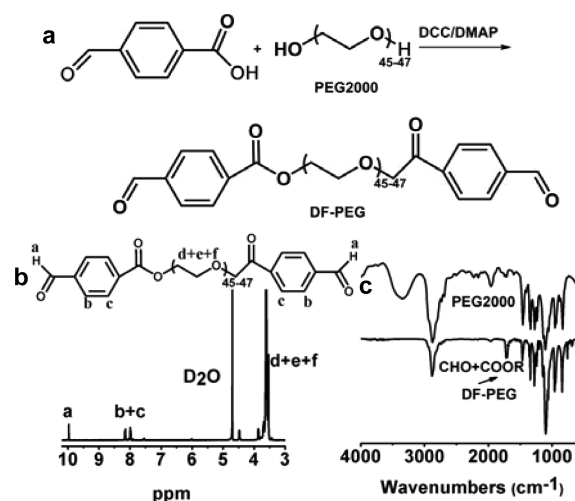


**Figure 1.** (a) Synthesis of DF-PEG. (b) <sup>1</sup>H NMR spectrum of DF-PEG in D<sub>2</sub>O. (c) FT-IR spectra of DF-PEG and PEG2000.

spectrum of DF-PEG, where peaks were observed at 9.98 and 7.98–8.21 ppm, which corresponded to aldehyde and aromatic group protons, respectively; the appearance of the former peak indicated the successful incorporation of benzaldehyde. The relative integration ratio of the peaks at 8.21, 7.98, 4.49, and 3.62 ppm was 4:4:4:183, which is close to the theoretical value of 4:4:4:174; this ratio indicates that all PEG hydroxyl groups are terminated with benzaldehyde groups. Figure 1c shows the FT-IR spectrum of DF-PEG; new bands were observed at 1719 and 1703 cm<sup>-1</sup>, corresponding to the absorption peaks of the ester and benzaldehyde groups, respectively, which is indicative of the successful modification of PEG with 4-formylbenzoic acid.

Meanwhile, hydrazine groups were introduced into PSI to prepare the other precursor polymer PAHy (Figure 2a). PAHy is a type of water-soluble, biocompatible polymer that has been widely used for the synthesis of macromolecular pro-drug<sup>42</sup> and polymeric hydrogels.<sup>43,44</sup> PAHy, which contains hydrazine side groups, was prepared from PSI.<sup>41</sup> As shown in Figure 2a, the ring opening of the five-membered imide ring of PSI occurs in the presence of hydrazine, resulting in the formation of a hydrazide group. The structure of PAHy was confirmed by <sup>1</sup>H NMR. Figure 2b shows the <sup>1</sup>H NMR spectrum of PAHy; clear signals were observed at 4.60 and 2.60–2.66 ppm, which correspond to the methine and methylene protons of the polymer, respectively. Figure 2c shows the FTIR spectra of PSI and PAHy; differences were observed in the 1700–1500 cm<sup>-1</sup> region. A single absorption peak was observed at  $\sim$ 1716 cm<sup>-1</sup> in the spectrum of PSI, which corresponds to the five-membered imide ring; on the other hand, in the spectrum of PAHy, two separated peaks were observed at 1645 and 1519

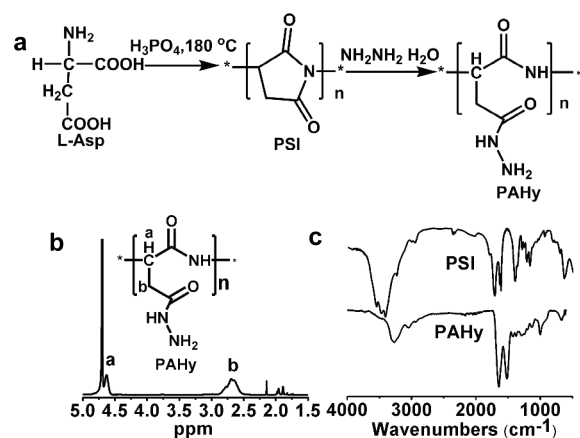


**Figure 2.** (a) Synthesis of PAHy. (b)  $^1\text{H NMR}$  spectrum of PAHy in  $D_2O$ . (c) FT-IR spectra of PAHy and PSI.

$\text{cm}^{-1}$ , which correspond to amide I and amide II of PAHy, respectively.

**Hydrogel Formation.** As shown in Figure 3a, the reaction between the hydrazine and benzaldehyde groups of PAHy and

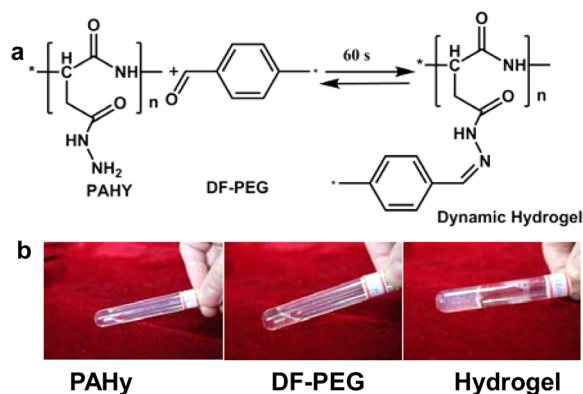


**Figure 3.** (a) Reaction equation of covalent cross-linked polymer hydrogel based on reversible covalent acylhydrazone bond. (b) Illustration of the state of gel precursors (PAHy and DF-PEG) and the hydrogel.

DF-PEG in an aqueous solution resulted in the formation of a hydrogel under neutral conditions by the formation of acylhydrazone bonds. The ester carbonyl of the aromatic ring was expected to stabilize the acylhydrazone bonds, which led to a rapid reaction between DF-PEG and PAHy and finally formed a hydrogel (Figure 3b). When equal volumes of DF-PEG and PAHy aqueous solutions were added to each other, a hydrogel rapidly formed, with almost complete gel formation during the mixing process ( $37\text{ }^\circ\text{C}$ ,  $<60\text{ s}$ ). To confirm the formation of cross-linking acylhydrazone bonds between PAHy and DF-PEG, FTIR spectroscopy was employed to characterize the prepared hydrogel (see Figure S1 in the Supporting Information; this figure shows the FTIR spectra of PAHy, DF-PEG, and the hydrogel). In the hydrogel FT-IR spectrum, the aldehyde absorption peaks of DF-PEG ( $1719$  and  $1703\text{ cm}^{-1}$ ) are absent. In comparison with that of PAHy, the IR spectrum of the hydrogel exhibited a shift in the amide I and II absorption peaks from  $1645$  and  $1519\text{ cm}^{-1}$  to  $1715$  and  $1667\text{ cm}^{-1}$ , respectively, demonstrating acylhydrazone bond formation. In this hydrogel, the molar ratio of  $\text{NH}_2\text{NH}_2/\text{CHO}$  is 1:1.08. To determine the efficiency of the reaction between the

hydrazide and aldehyde groups, the amount of unreacted hydrazides was indirectly calculated by TNBS assay.<sup>45</sup> The efficiency of the hydrazone cross-linking reaction in the hydrogels is  $\sim 74.9\%$ .

#### pH-Responsive Ability of the Injectable Hydrogel.

Figure 4 shows the reversibility of the sol–gel transitions of the

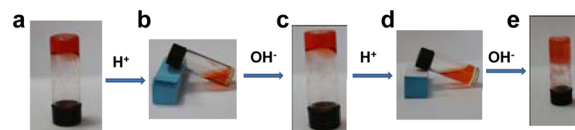


**Figure 4.** Hydrogel phase transitions by changing pH values: (a) gel state, (b) sol state when concentrated HCl was added, (c) recovery of the gel state when NaOH solution was added, (d) dissolution of the regenerated gel when concentrated HCl was included again, and (e) the gel after five cycles of regeneration.

prepared hydrogel in response to pH changes. Trace DOX has also been shown for better observation. Typically, acylhydrazone bonds can be easily hydrolyzed in an acidic medium. As expected, by the addition of concentrated HCl, the prepared hydrogel was decomposed in  $\sim 15$  min (Figures 4a and 4b). Moreover, after the addition of the NaOH solution, the gel was recovered within  $<60\text{ s}$  (Figure 4c). This process was repeated five times (Figures 4d and 4e), indicating the reversible formation and decomposition of the prepared hydrogel. The regenerated gel was opaque caused by formation of sodium chloride precipitates formed as a result of acid–base neutralization.<sup>24</sup>

**In Vitro Biodegradability of the pH-Responsive Hydrogel.** The pH-responsive moiety, the acylhydrazone bond, is typically sensitive to hydrolysis under acidic condition. Typically, this process is rapid and enables the hydrogel to degrade rapidly. To investigate the external and internal morphologies of the hydrogels under different pH conditions, scanning electron microscopy (SEM) images of the hydrogels were recorded. Figure 5a shows the hydrogel prepared after

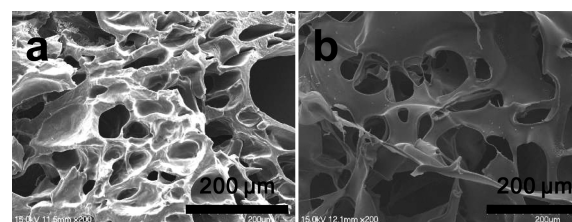


**Figure 5.** (a) SEM image of the prepared hydrogel at pH 7.4. (b) SEM image of the prepared hydrogel immersed in a pH 6.0 buffer after 48 h.

immersion in PBS ( $10\text{ mM}$ , pH 7.4); a porous 3D structure was observed, which is important for drug loading. Intermolecular acylhydrazone bonds between aldehydes and hydrazines are key bonds for forming a stable gel. However, after treatment with a buffer of pH 6, the hydrogels demonstrated varying pore sizes, with all being greater than those of the pristine hydrogel (Figure 5b). This is probably due to the cleavage of the acylhydrazone bonds under acidic conditions, resulting in the decomposition of the hydrogel structure, which, in turn, makes it significantly easier for the hydrogel to degrade and release the drug. In addition to SEM, a rheology study was expected to be useful in demonstrating the hydrolytic degradability of the hydrogels. Hence, we quantified the storage modulus in all

experiments as a measure of the extent of intermolecular cross-linking. Figure S2 in the Supporting Information shows the rheology data before and after the incubation of the hydrogels at different pH values. We found that decreasing pH values resulted in a decrease of the storage modulus of the cross-linked hydrogels, which is consistent with the SEM results.

**DOX Loading and *In Vitro* DOX Release.** Considering the acidic nature of the intracellular endocytic vesicles and tumor extracellular sites, the DOX release profile from the pH-responsive hydrogel was observed after treating the DOX-loaded hydrogel samples at a series of pH values. In the DOX-loaded hydrogels, the molar ratio of PAHy hydrazide groups, DF-PEG aldehyde groups, and DOX is  $\sim 1:1.08:2.96$ . Based on this molar ratio, we rationalized that there could be three immobilized forms of DOX in the hydrogel: (i) physically encapsulated DOX, (ii) Schiff base linkages between DF-PEG aldehyde groups and DOX amine groups,<sup>46</sup> and (iii) hydrazone linkages between PAHy hydrazide groups and DOX carbonyl groups.<sup>47</sup> Figure S3 in the Supporting Information shows the DOX release profiles of free DOX, the DOX + PAHy mixture, and the DOX + DF-PEG mixture under different pH conditions. From the profiles, the release of DOX from each of the three immobilized forms is dependent on pH. The profiles in Figure S3 in the Supporting Information also demonstrate that the release of DOX from hydrazone linkages is slightly more sensitive than that from Schiff base linkages. Figure 6 shows the drug release profiles of the DOX-loaded

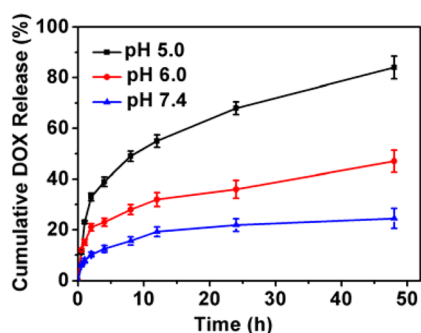


**Figure 6.** DOX release from the injectable hydrogel under different pH mediums.

hydrogels under various pH conditions; differences indicate that drug release is significantly pH-responsive. As shown in Figure 6, the DOX release rate from the pH-responsive hydrogel consistently increased with decreasing pH (from pH 7.4 to pH 5.0). Only a small amount of DOX release was observed at pH 7.4, which corresponds to the physiological conditions of the bloodstream. Thus, marginal DOX is expected to be released from the hydrogel under normal physiological conditions, which is a desirable characteristic for the drug carrier in drug delivery systems. The results also indicate that, at physiological pH, the hydrogel is stable for a long period of time. At pH 5.0 and 6.0, DOX release was 84% and 47%, respectively, in 48 h, while only 24.5% of DOX was released from the DOX-loaded hydrogel at pH 7.4 during the same time period. This is due to the cleavage of acylhydrazone bonds in the acidic environment to release DOX. At lower pH, more acylhydrazone bonds were broken than at higher pH. Thus, once the hydrogel is injected into the tumor tissue, the encapsulated DOX should be effectively released to improve the therapeutic outcome of chemotherapy.

**Biocompatibility Evaluation.** To act as an effective vehicle for the drug in a drug delivery system, the hydrogel must be nontoxic to the normal body cells. NIH-3T3 and HT1080 cells were used to investigate the preliminary cytotoxicity of the DOX-free hydrogel based on the MTT assay. In the investigation, we first treated the cells with different concentrations of the empty hydrogel solution and then incubated them for 48 h. As shown in Figure 7, the result

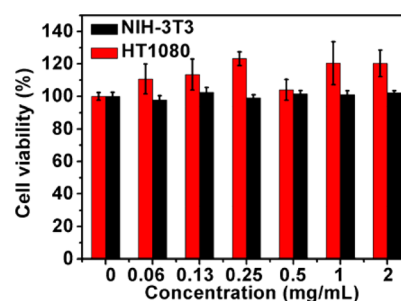


**Figure 7.** Biocompatibility of the injectable hydrogel to NIH-3T3 and HT1080 cells after incubation for 48 h.

(regardless of whether NIH-3T3 or HT1080 cells are used) clearly indicated that more than 95% of cells are viable, even at the highest concentration (2 mg/mL) of the dilute hydrogel solution presented. These data show that the pH-responsive hydrogel is nontoxic, suggesting that the prepared hydrogel demonstrates promise for *in vivo* applications.

**Evaluation of Gel Formation *In Vivo*.** To evaluate the *in vivo* formation of the pH-responsive hydrogels, the precursor solutions were injected into the subcutaneous tissue of a BALB/c mouse. As shown in Figure 8A, a hydrogel was



**Figure 8.** Evaluation of gel formation *in vivo*: photographs were taken 10 min after injection of the precursors (PAHy and DF-PEG) solution into mice.

subcutaneously formed 10 min after the injection of the precursor PAHy and DF-PEG solutions. The experiment indicates that the precursor PAHy and DF-PEG solutions can be easily injected *in vivo* and that they form a hydrogel within a short time.

**Antitumor Efficacy of the DOX-Loaded Hydrogel.** To demonstrate the *in vivo* drug delivery efficacy of the hydrogel via the pH-responsive effect, the DOX-loaded hydrogel was intratumorally injected into nude mice bearing HT1080 tumors. The antitumor efficacy of the DOX-loaded hydrogel was compared with that of the free DOX solution (Figure 9). The DOX-loaded hydrogel exhibited antitumor activity superior than that of free DOX solution, suggesting the importance of the controlled release, while a saline control group exhibited negligible antitumor activity (Figure 9a). The tumor volume in the control group changed to 1.5 times on the sixth day compared with that on the zeroth day, while progression to this tumor volume was delayed to the 20th day by free DOX. On the other hand, for the group treated by the DOX-loaded hydrogel, the mean tumor volume was signifi-

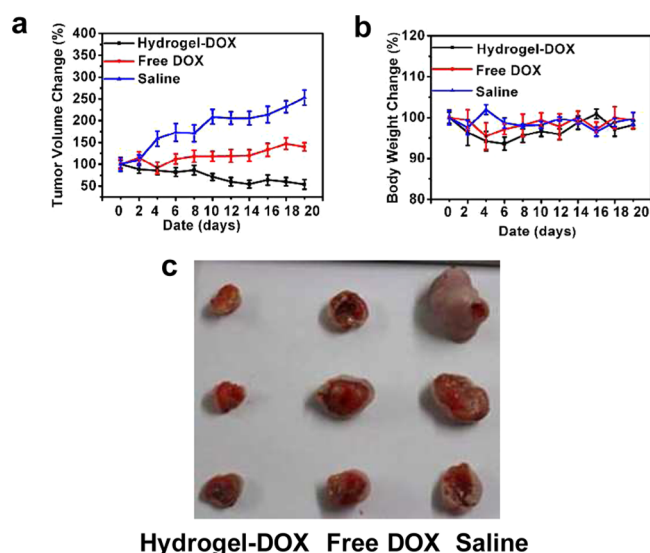


**Figure 9.** (a) *In vivo* tumor volume change curves of tumor-bearing mice as a function of time. (b) Body weight change curves of tumor-bearing mice as a function of time. (c) Typical images of excised tumors from mice on the 20th day. Data are presented as mean  $\pm$  SD ( $n = 3$ ).

cantly inhibited and only 0.5 times of the original tumor volume was observed even on the 20th day (Figure 9a). These results clearly showed that DOX is significantly retained intratumorally when encapsulated into the hydrogel in comparison to free DOX. A relative change in body weight was recorded during the experiments to evaluate the health status of mice (Figure 9b). As shown in Figure 9b, the body weight of mice treated with the DOX-loaded hydrogel and free DOX solution was not significantly different, compared to that of the control group. This observation suggests that the treatment with the DOX-loaded hydrogel is tolerated well with negligible toxicity. At the end of the treatment, the tumors were excised as shown in Figure 9c. The DOX-loaded hydrogel showed tumor inhibition higher than that exhibited by the free DOX solution. These results demonstrate that the DOX-loaded hydrogel has significant antitumor activity against HT1080 xenografts.

**Histological Analysis.** To investigate the antitumor activity of the DOX-loaded hydrogel further, nude mice bearing the HT1080 tumor were sacrificed after the treatment (day 20) and the tumors were dissected, fixed and stained with H&E for pathological analysis. Figure 10 shows the data of the groups treated with saline, free DOX and the DOX-loaded hydrogel. As shown in Figure 10, the normal tumor cells exhibited large nuclei with spherical or spindle shapes, while the apoptotic cells did not exhibit a clear cytoskeleton. In addition, clear separation was observed between nuclei and the cytoplasm in necrotic or

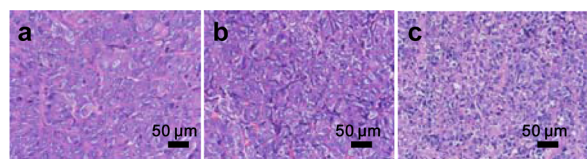


**Figure 10.** H&E staining of tumor sections collected from different groups of mice treated with (a) saline, (b) free DOX, and (c) the DOX-loaded hydrogel.

apoptotic cells. By contrast, tumor cells with normal shapes and large nuclei were observed in the saline group, revealing vigorous tumor growth (Figure 10). However, various degrees of tissue necrosis with nuclei or cytosol separation were observed in the different drug-formulation-treated groups. The tumors of the DOX-loaded-hydrogel-treated group exhibited larger necrosis areas, compared with those of the group treated with free DOX, indicating that most tumor cells are necrotic in the group treated with the DOX-loaded hydrogel.

## CONCLUSIONS

In this study, a simple, efficient procedure was adopted to synthesize a pH-responsive hydrogel using dibenzaldehyde-functionalized PEG and  $\alpha,\beta$ -polyaspartylhydrazide as the raw materials. Specifically, the hydrogel network was created by the generation of dynamic acylhydrazone linkages between hydrazide sites on the poly(aspartic acid) backbone and terminal benzaldehyde sites on the PEG chain. The pH-responsive hydrogel was characterized and used to load doxorubicin (DOX) for local cancer chemotherapy. Scanning electron microscopy images of the hydrogel showed a three-dimensional structure, which enabled the slow and steady release of DOX. In mice with human fibrosarcoma, the rate of release of DOX encapsulated by the hydrogel and accumulation inside the tumor were obviously slower than those of free DOX. Therefore, the DOX-loaded hydrogel had a greater effect than free DOX, and  $\sim 80\%$  complete inhibition of tumors was observed on day 20. Therefore, the DOX-loaded hydrogel can be potentially used as a highly efficient medicine for the chemotherapy of human fibrosarcoma with significantly minimized side effects.

## ASSOCIATED CONTENT

### Supporting Information

Additional information as noted in text, including FT-IR spectra of PAHy, DF-PEG, and hydrogel; storage shear moduli ( $G'$ ) as a function of angular frequency ( $\omega$ ) for the hydrogels under various pH conditions; *in vitro* release of DOX from free DOX, the PAHy + DOX mixture, and the DF-PEG + DOX mixture under different pH media. This material is available free of charge via the Internet at <http://pubs.acs.org>.

## AUTHOR INFORMATION

### Corresponding Authors

\*Tel.: 86-512-67784117. E-mail: [dqr@szgk.net](mailto:dqr@szgk.net) (Q. Dong).

\*Tel.: 86-512-65882263. E-mail: [yywang578@suda.edu.cn](mailto:yywang578@suda.edu.cn) (Y. Wang).

### Author Contributions

#These authors contributed equally.

### Notes

The authors declare no competing financial interest.

## ACKNOWLEDGMENTS

This work was supported by a project funded by the Priority Academic Program Development of Jiangsu Higher Education Institutions, Jiangsu Provincial Key Laboratory of Radiation Medicine and Protection, the Postdoctoral Research Program of Jiangsu Province (No. 1402109C), Sports Scientific Research Bureau Program of Suzhou Sports Bureau (No. TY2014-202), Youth Research Institute Foundation of the Second Affiliated Hospital of Soochow University (Nos. SDFEYQN1401 and

SDFEYQN1411), and the National Natural Science Foundation of China (No. K112824214).

## REFERENCES

- (1) Yan, S.; Wang, T.; Feng, L.; Zhu, J.; Zhang, K.; Chen, X.; Cui, L.; Yin, J. Injectable *In Situ* Self-Cross-Linking Hydrogels Based on Poly(L-glutamic acid) and Alginate for Cartilage Tissue Engineering. *Biomacromolecules* **2014**, *15*, 4495–4508.
- (2) Mehdizadeh, M.; Weng, H.; Gyawali, D.; Tang, L.; Yang, J. Injectable Citrate-Based Mussel-Inspired Tissue Bioadhesives with High Wet Strength for Sutureless Wound Closure. *Biomaterials* **2012**, *33*, 7972–7983.
- (3) Ni, P.; Ding, Q.; Fan, M.; Liao, J.; Qian, Z.; Luo, J.; Li, X.; Luo, F.; Yang, Z.; Wei, Y. Injectable Thermosensitive PEG-PCL-PEG Hydrogel/Acellular Bone Matrix Composite for Bone Regeneration in Cranial Defects. *Biomaterials* **2014**, *35*, 236–248.
- (4) Huebsch, N.; Kearney, C. J.; Zhao, X.; Kim, J.; Cezar, C. A.; Suo, Z.; Mooney, D. J. Ultrasound-Triggered Disruption and Self-Healing of Reversibly Cross-Linked Hydrogels for Drug Delivery and Enhanced Chemotherapy. *Proc. Natl. Acad. Sci. U. S. A.* **2014**, *111*, 9762–9767.
- (5) Wu, W.; Chen, H.; Shan, F.; Zhou, J.; Sun, X.; Zhang, L.; Gong, T. A Novel Doxorubicin-Loaded *In Situ* Forming Gel Based High Concentration of Phospholipid for Intratumoral Drug Delivery. *Mol. Pharmaceutics* **2014**, *11*, 3378–3385.
- (6) Kean, Z. S.; Hawk, J. L.; Lin, S.; Zhao, X.; Sijbesma, R. P.; Craig, S. L. Increasing the Maximum Achievable Strain of a Covalent Polymer Gel through the Addition of Mechanically Invisible Cross-Links. *Adv. Mater.* **2014**, *26*, 6013–6018.
- (7) Huang, Y.; Lawrence, P. G.; Lapitsky, Y. Self-Assembly of Stiff, Adhesive and Self-Healing Gels from Common Polyelectrolytes. *Langmuir* **2014**, *30*, 7771–7777.
- (8) Kloxin, C. J.; Bowman, C. N. Covalent Adaptable Networks: Smart, Reconfigurable and Responsive Network Systems. *Chem. Soc. Rev.* **2013**, *42*, 7161–7173.
- (9) Park, M. R.; Seo, B. B.; Song, S. C. Dual Ionic Interaction System Based on Polyelectrolyte Complex and Ionic, Injectable, and Thermosensitive Hydrogel for Sustained Release of Human Growth Hormone. *Biomaterials* **2013**, *34*, 1327–1336.
- (10) Seo, H. W.; Kim da, Y.; Kwon, D. Y.; Kwon, J. S.; Jin, L. M.; Lee, B.; Kim, J. H.; Min, B. H.; Kim, M. S. Injectable Intratumoral Hydrogel as 5-Fluorouracil Drug Depot. *Biomaterials* **2013**, *34*, 2748–2757.
- (11) Li, L.; Yan, B.; Yang, J.; Chen, L.; Zeng, H. Novel Mussel-Inspired Injectable Self-Healing Hydrogel with Anti-Biofouling Property. *Adv. Mater.* **2015**, *27*, 1294–1299.
- (12) Kim, J. I.; Kim, D. Y.; Kwon, D. Y.; Kang, H. J.; Kim, J. H.; Min, B. H.; Kim, M. S. An Injectable Biodegradable Temperature-Responsive Gel with An Adjustable Persistence Window. *Biomaterials* **2012**, *33*, 2823–2834.
- (13) Popescu, M. T.; Tsitsilianis, C.; Papadakis, C. M.; Adelsberger, J.; Balog, S.; Busch, P.; Hadjiantoniou, N. A.; Patrickios, C. S. Stimuli-Responsive Amphiphilic Polyelectrolyte Heptablock Copolymer Physical Hydrogels: An Unusual pH-Response. *Macromolecules* **2012**, *45*, 3523–3530.
- (14) Yang, X.; Cranston, E. D. Chemically Cross-Linked Cellulose Nanocrystal Aerogels with Shape Recovery and Superabsorbent Properties. *Chem. Mater.* **2014**, *26*, 6016–6025.
- (15) Wei, H.-L.; Yang, Z.; Zheng, L.-M.; Shen, Y.-M. Thermosensitive Hydrogels Synthesized by Fast Diels–Alder Reaction in Water. *Polymer* **2009**, *50*, 2836–2840.
- (16) Weng, L.; Romanov, A.; Rooney, J.; Chen, W. Non-Cytotoxic, *In Situ* Gelable Hydrogels Composed of N-Carboxyethyl Chitosan and Oxidized Dextran. *Biomaterials* **2008**, *29*, 3905–3913.
- (17) Nishi, K. K.; Jayakrishnan, A. Self-Gelling Primaquine-Gum Arabic Conjugate: An Injectable Controlled Delivery System for Primaquine. *Biomacromolecules* **2006**, *8*, 84–90.
- (18) Deng, G.; Tang, C.; Li, F.; Jiang, H.; Chen, Y. Covalent Cross-Linked Polymer Gels with Reversible Sol–Gel Transition and Self-Healing Properties. *Macromolecules* **2010**, *43*, 1191–1194.
- (19) Arnold, R. M.; Patton, D. L.; Popik, V. V.; Locklin, J. A Dynamic Duo: Pairing Click Chemistry and Postpolymerization Modification To Design Complex Surfaces. *Acc. Chem. Res.* **2014**, *47*, 2999–3008.
- (20) Li, W.; Dong, Z.; Zhu, J.; Luo, Q.; Liu, J. Spontaneous Formation of Organic Helical Architectures Through Dynamic Covalent Chemistry. *Chem. Commun. (Cambridge, U.K.)* **2014**, *50*, 14744–14747.
- (21) Imato, K.; Ohishi, T.; Nishihara, M.; Takahara, A.; Otsuka, H. Network Reorganization of Dynamic Covalent Polymer Gels with Exchangeable Diarylbibenzofuranone at Ambient Temperature. *J. Am. Chem. Soc.* **2014**, *136*, 11839–11845.
- (22) Ji, S.; Cao, W.; Yu, Y.; Xu, H. Dynamic Diselenide Bonds: Exchange Reaction Induced by Visible Light without Catalysis. *Angew. Chem., Int. Ed.* **2014**, *53*, 6781–6785.
- (23) Jin, Y.; Wang, Q.; Taynton, P.; Zhang, W. Dynamic Covalent Chemistry Approaches Toward Macrocycles, Molecular Cages, and Polymers. *Acc. Chem. Res.* **2014**, *47*, 1575–1586.
- (24) Zhang, Y.; Tao, L.; Li, S.; Wei, Y. Synthesis of Multiresponsive and Dynamic Chitosan-Based Hydrogels for Controlled Release of Bioactive Molecules. *Biomacromolecules* **2011**, *12*, 2894–2901.
- (25) Zhang, Y.; Yang, B.; Zhang, X.; Xu, L.; Tao, L.; Li, S.; Wei, Y. A Magnetic Self-Healing Hydrogel. *Chem. Commun. (Cambridge, U.K.)* **2012**, *48*, 9305–9307.
- (26) Yang, B.; Zhang, Y.; Zhang, X.; Tao, L.; Li, S.; Wei, Y. Facilely Prepared Inexpensive and Biocompatible Self-Healing Hydrogel: A New Injectable Cell Therapy Carrier. *Polym. Chem.* **2012**, *3*, 3235–3238.
- (27) Bouillon, C.; Paolantoni, D.; Rote, J. C.; Bessin, Y.; Peterson, L. W.; Dumy, P.; Ulrich, S. Degradable Hybrid Materials Based on Cationic Acylhydrazone Dynamic Covalent Polymers Promote DNA Complexation through Multivalent Interactions. *Chem.—Eur. J.* **2014**, *20*, 14705–14714.
- (28) Yu, J.; Deng, H.; Xie, F.; Chen, W.; Zhu, B.; Xu, Q. The Potential of pH-Responsive PEG-Hyperbranched Polyacylhydrazone Micelles for Cancer Therapy. *Biomaterials* **2014**, *35*, 3132–3144.
- (29) Corbett, P. T.; Leclaire, J.; Vial, L.; West, K. R.; Wietor, J.-L.; Sanders, J. K. M.; Otto, S. Dynamic Combinatorial Chemistry. *Chem. Rev.* **2006**, *106*, 3652–3711.
- (30) Bhat, V. T.; Caniard, A. M.; Luksch, T.; Brenk, R.; Campopiano, D. J.; Greaney, M. F. Nucleophilic Catalysis of Acylhydrazone Equilibration for Protein-Directed Dynamic Covalent Chemistry. *Nat. Chem.* **2010**, *2*, 490–497.
- (31) Deng, G.; Li, F.; Yu, H.; Liu, F.; Liu, C.; Sun, W.; Jiang, H.; Chen, Y. Dynamic Hydrogels with an Environmental Adaptive Self-Healing Ability and Dual Responsive Sol–Gel Transitions. *ACS Macro Lett.* **2012**, *1*, 275–279.
- (32) Kepka, L.; DeLaney, T. F.; Suit, H. D.; Goldberg, S. I. Results of Radiation Therapy for Unresected Soft-Tissue Sarcomas. *Int. J. Radiat. Oncol. Biol. Phys.* **2005**, *63*, 852–859.
- (33) Pratt, C. B.; Maurer, H. M.; Gieser, P.; Salzberg, A.; Rao, B. N.; Parham, D.; Thomas, P. R. M.; Marcus, R. B.; Cantor, A.; Pick, T.; Green, D.; Neff, J.; Jenkins, J. J. Treatment of Unresectable or Metastatic Pediatric Soft Tissue Sarcomas with Surgery, Irradiation, and Chemotherapy: A Pediatric Oncology Group Study. *Med. Pediatr. Oncol.* **1998**, *30*, 201–209.
- (34) Altunbas, A.; Lee, S. J.; Rajasekaran, S. A.; Schneider, J. P.; Pochan, D. J. Encapsulation of Curcumin in Self-Assembling Peptide Hydrogels as Injectable Drug Delivery Vehicles. *Biomaterials* **2011**, *32*, 5906–5914.
- (35) Lee, C.-M.; Kwon, J.-I.; Lee, T.-K.; Lim, S. T.; Sohn, M.-H.; Jeong, H.-J. Local Retention and Combination Effects of Biocompatible Doxorubicin-Loaded and Radioiodine-Labeled Microhydrogels in Cancer Therapy. *ACS Macro Lett.* **2014**, *3*, 1126–1129.
- (36) Nance, E.; Zhang, C.; Shih, T.-Y.; Xu, Q.; Schuster, B. S.; Hanes, J. Brain-Penetrating Nanoparticles Improve Paclitaxel Efficacy in Malignant Glioma Following Local Administration. *ACS Nano* **2014**, *8*, 10655–10664.
- (37) Peng, C.-L.; Shih, Y.-H.; Liang, K.-S.; Chiang, P.-F.; Yeh, C.-H.; Tang, I. C.; Yao, C.-J.; Lee, S.-Y.; Luo, T.-Y.; Shieh, M.-J. Development

of In Situ Forming Thermosensitive Hydrogel for Radiotherapy Combined with Chemotherapy in a Mouse Model of Hepatocellular Carcinoma. *Mol. Pharmaceutics* **2013**, *10*, 1854–1864.

(38) Wang, X. J.; Wu, G. L.; Lu, C. C.; Zhao, W. P.; Wang, Y. N.; Fan, Y. G.; Gao, H.; Ma, J. B. A Novel Delivery System of Doxorubicin With High Load and pH-Responsive Release from the Nanoparticles of Poly(Alpha,Beta-Aspartic Acid) Derivative. *Eur. J. Pharm. Sci.* **2012**, *47*, 256–264.

(39) Wang, X. J.; Wu, G. L.; Lu, C. C.; Wang, Y. N.; Fan, Y. G.; Gao, H.; Ma, J. B. Synthesis of A Novel Zwitterionic Biodegradable Poly (Alpha,Beta-L-Aspartic Acid) Derivative with Some L-Histidine Side-Residues and Its Resistance to Non-Specific Protein Adsorption. *Colloids Surf, B* **2011**, *86*, 237–241.

(40) Licciardi, M.; Cavallaro, G.; Di Stefano, M.; Pitarresi, G.; Fiorica, C.; Giammona, G. New Self-Assembling Polyaspartylhydrazide Copolymer Micelles for Anticancer Drug Delivery. *Int. J. Pharm.* **2010**, *396*, 219–228.

(41) Lu, C. C.; Wang, X. J.; Wu, G. L.; Wang, J. J.; Wang, Y. N.; Gao, H.; Ma, J. B. An Injectable and Biodegradable Hydrogel Based on Poly(Alpha,Beta-Aspartic Acid) Derivatives for Localized Drug Delivery. *J. Biomed. Mater. Res., Part A* **2014**, *102*, 628–638.

(42) Giammona, G.; Carlisi, B.; Cavallaro, G.; Pitarresi, G.; Spampinato, S. A New Water-Soluble Synthetic Polymer,  $\alpha,\beta$ -Polyasparthydrazide, as Potential Plasma Expander and Drug Carrier. *J. Controlled Release* **1994**, *29*, 63–72.

(43) Paolino, D.; Cosco, D.; Licciardi, M.; Giammona, G.; Fresta, M.; Cavallaro, G. Polyaspartylhydrazide Copolymer-Based Supramolecular Vesicular Aggregates as Delivery Devices for Anticancer Drugs. *Biomacromolecules* **2008**, *9*, 1117–1130.

(44) Pitarresi, G.; Cavallaro, G.; Carlisi, B.; Giammona, G.; Bulone, D.; San Biagio, P. L. Novel Hydrogels Based on a Polyasparthydrazide. Synthesis and Characterization. *Macromol. Chem. Phys.* **2000**, *201*, 2542–2549.

(45) Lee, K. Y.; Bouhadir, K. H.; Mooney, D. J. Degradation Behavior of Covalently Cross-Linked Poly(aldehyde guluronate) Hydrogels. *Macromolecules* **1999**, *33*, 97–101.

(46) Saito, H.; Hoffman, A. S.; Ogawa, H. I. Delivery of Doxorubicin from Biodegradable PEG Hydrogels Having Schiff Base Linkages. *J. Bioact. Compat. Polym.* **2007**, *22*, 589–601.

(47) Ossipov, D.; Kootala, S.; Yi, Z.; Yang, X.; Hilborn, J. Orthogonal Chemoselective Assembly of Hyaluronic Acid Networks and Nanogels for Drug Delivery. *Macromolecules* **2013**, *46*, 4105–4113.